Annu. Rev. Astron. Astrophys. 1990. 28:657–88

THE SOFT X-RAY BACKGROUND AND ITS ORIGINS

Dan McCammon and Wilton T. Sanders

Physics Department, University of Wisconsin, Madison, Wisconsin 53706

KEY WORDS: X rays, diffuse background, interstellar medium, galaxies

1. *Introduction*

The sky in the soft X-ray region of the electromagnetic spectrum (photon energies between roughly 0.1 and 10 keV) is far from dark: Over this entire energy range, the diffuse flux is much greater than the contribution from identifiable discrete sources. It now appears that there are several diffuse X-ray backgrounds, and despite the title of this review, we are not all that sure of the origin of any of them.

Soft X rays are an energetic phenomenon. Thermal production over this energy range requires temperatures in the range 10^6–10^8 K. Nonthermal processes require 50–500 GeV electrons for synchrotron radiation in a typical galactic magnetic field, 5–50 MeV electrons for inverse Compton scattering of starlight photons, and 300–3000 MeV electrons for inverse Compton on microwave background photons.

The dominant interaction with matter for X rays below 10 keV is photoelectric absorption. This cross section increases rapidly at lower energies, scaling approximately as E^{-3}. As shown in Figure 1, this results in a range of mean free paths in an assumed average interstellar density of 1 H atom cm^{-3} that encompasses the entire range of galactic distance scales. At 0.1 keV, X rays would barely reach us from neighboring stars (although the use of an average density here is certainly not correct), whereas at 10 keV the entire diameter of the disk is transparent. Interstellar scattering can be ignored over the entire energy range. The sharp jumps

0066–4146/90/0915–0657$02.00

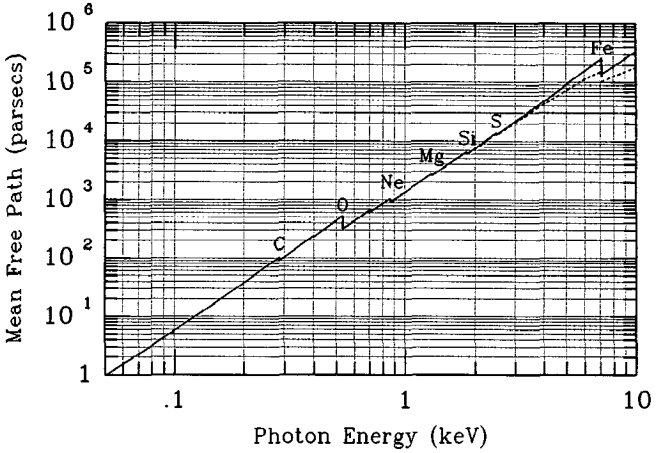

Figure 1 Interstellar mean free path at an assumed average density of 1 H atom cm^{-3} and assumed solar abundances. The solid line is photoelectric absorption only, whereas the dashed line includes Thomson scattering. Elements responsible for the major absorption edges are indicated. Data are from (88).

in the mean free path are caused by atomic absorption edges of the more abundant heavy elements. These provide an opportunity for direct measurement of interstellar column densities of particular species.

Diffuse X rays were one of the first discoveries of X-ray astronomy. In 1962, a sounding rocket carrying Geiger counters sensitive in the 2–6 keV range observed both the first "X-ray star," Scorpius X-1, and a copious isotropic flux (36). The observed isotropy implies that the origin is either very local or very distant, since all known material in the Galaxy is distributed quite anisotropically as viewed from the Sun. The lack of interstellar absorption at these energies means that there is nothing to restrict our view to a local source, so only an extragalactic origin seems possible. This was an exciting discovery, as it was the first cosmological diffuse flux ever observed. It was followed a few years later by the discovery of the cosmic microwave background by Penzias & Wilson (96), and these remain the only regions of the electromagnetic spectrum where extragalactic diffuse radiation is not overwhelmed by local sources. Further observations have shown that the photon flux extends to at least 100 MeV (31, 71), where it is dominated by the harder spectrum of galactic diffuse emission produced through interactions of cosmic rays with interstellar material (5).

There are a number of theories for the origin of the extragalactic component of the radiation. The integrated emission from active galactic nuclei

probably contributes significantly to it and could conceivably account for all of the flux (37, 87a). On the other hand, thermal bremsstrahlung from a thin intergalactic plasma with $kT = \sim 40$ keV provides an excellent fit to the observed spectrum from 3 to 50 keV (79). There are difficulties with both of these models, however, and some unknown population of sources at large redshifts may be responsible for the bulk of the flux (116, and references therein).

Soon after the discovery of the soft X-ray background flux, it was speculated that when instruments capable of observing the extragalactic flux below 1 keV were developed, one could study the distribution of interstellar material in the Galaxy by looking at the patterns of absorption. In effect, the isotropic background could be used as a source to "x-ray" the interstellar medium. The first successful measurement in this energy range was reported by Bowyer et al in 1968 (10). The observed flux at low energies decreased as expected at low galactic latitudes, where the interstellar absorption of an extragalactic source should be greater. Shortly thereafter, it was noted that the absolute intensity of the flux far exceeded an extrapolation of the spectrum observed above 2 keV (49). At that time it seemed natural to interpret this excess as another component of the extragalactic flux. A particularly attractive proposition attributed it to thermal radiation from an intergalactic plasma at a density somewhat larger than the critical value required to close the Universe. The inferred temperature, about 10^6 K, was within the narrow allowed range for such a dense medium, bounded below by the lack of Lα absorption continua in quasar spectra, and above by the requirement that its thermal radiation not exceed the X-ray flux observed above 2 keV (131). As discussed below, observational details never really favored this interpretation, but the theoretical attractiveness of the model and the lack of reasonable alternatives kept it alive for a number of years.

It is now generally thought that the excess below 0.25 keV is due to thermal radiation from a 10^6-K component of the interstellar gas in our Galaxy, and that most of it originates within a few hundred parsecs of the Sun. The degree of pervasiveness of such hot gas in the galactic disk is unknown, but the possibility that it is common has dramatically altered our view of the structure and evolution of the interstellar medium (ISM). Since 10^6-K gas can most easily be detected through its X-ray emission, diffuse soft X-ray observations have indeed become an important tool for studying the ISM, although not in the mode originally envisioned.

This review is concerned primarily with diffuse galactic emission. However, in the intermediate energy range (0.5–1 keV) it is not yet clear just how much of the observed radiation is galactic or extragalactic, so we cannot entirely isolate this subject. Even where it can be shown that almost

all of the detected X rays are galactic, this is not the same thing as saying that there are no extragalactic X rays. The great intrinsic interest of extragalactic "background light" levels at any wavelength makes it worth using what understanding we have of the foreground emission to extract as much information as possible about the value of the extragalactic flux. Current limits and the prospects for improving them are discussed in Section 6.

A number of good reviews exist for observations of the extragalactic diffuse X-ray background and its interpretation (7, 37, 39, 75, 113, 116, 117). Of the previous reviews of the galactic diffuse emission (23, 105, 124), we particularly recommend the encyclopedic 1977 review by Tanaka & Bleeker (124). For many areas, it provides a more detailed discussion than we can include here, and it is a good reference to many of the important early experiments. In most cases Tanaka & Bleeker reached the same conclusions that we do here, although a good deal of intuition and taste were required on their part to extract these from the more limited and conflicting data available at that time.

2. *Emission Mechanisms for the Galactic Diffuse Background*

Several authors have considered whether the soft X-ray background could arise from the superposition of point sources or if it must be truly diffuse (12, 38, 76, 128). The low level of intensity fluctuations of the 0.25-keV background implies a space density of point source emitters of at least 0.2 pc^{-3}, greater than that of all stars. Stellar X-ray luminosity functions measured using the *Einstein* satellite (19, 47, 104; J. Schmitt & S. Snowden, private communication) predict that normal stars of all types produce less than a few percent of the observed 0.25-keV diffuse background and no more than 20% of the 0.5–1.0 keV flux.

Several diffuse nonthermal mechanisms have been considered to explain the soft X-ray background and have been rejected because they predict other effects that are not observed (40, 70, 132). The electron flux needed for soft X-ray production by bremsstrahlung on interstellar gas or inverse Compton scattering from starlight would produce much more ionization of the interstellar gas than is allowed. Electrons capable of producing the soft X-ray background by inverse Compton scattering from the 3-K microwave background or as transition radiation from collisions with dust would also produce a flux of 100-MeV gamma rays much larger than is observed. Electrons energetic enough to produce soft X-rays by the synchrotron process in the galactic field would lose half their energy on a time scale of 5000 yr.

Diffuse thermal emission at temperatures of $\sim 10^6$ K remains as the probable source of the 0.25-keV X-ray background, and at 2–4 $\times$ 10^6 K

it may well be responsible for most of the galactic emission in the 0.5–1.0 keV range. Direct evidence for hot interstellar gas at slightly lower temperatures has come from the *Copernicus* observations of O VI absorption (59–61). Radiation from plasmas in the 0.5–4 $\times$ 10^6 K range is entirely dominated by collisionally excited emission lines of the partially ionized heavy elements ($Z \geq 5$). Figure 2 shows calculated X-ray emission spectra for gas with solar abundances in collisional equilibrium at temperatures in the range 10^5–10^7 K (98; see also 66, 87, 99, 99a, 123). Times required for such plasmas to reach collisional equilibrium can be long compared with heating and cooling time scales, so considerable work has been done

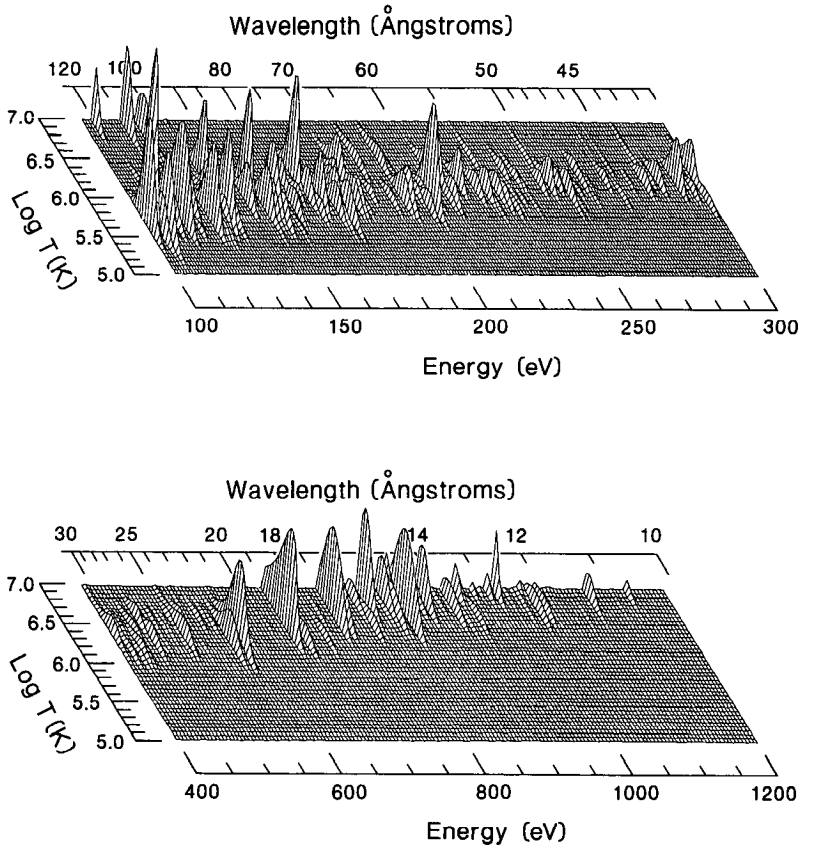

Figure 2 Calculated X-ray emission for an optically thin plasma with solar abundances in collisional equilibrium (98). Spectra are shown as a function of the gas temperature from 10^5 to 10^7 K. The vertical scales are linear in photon emissivity.

also on calculations for various nonequilibrium situations (1, 22, 29, 50, 119, 120a).

While high-resolution spectroscopy of the diffuse X-ray background is currently in its infancy, there is clearly a wealth of information potentially available on the detailed physical conditions in these hot regions of the ISM. Not only can temperature distributions and elemental abundances be measured with precision, but it should also be possible to determine much about the past history of the gas, including the time elapsed since it was heated.

3. *Observations*

INSTRUMENTATION The Geiger counters of the first rocket flights were soon replaced with proportional counters, for which the amplitude of the signal pulses is proportional to the energy of the absorbed photon. The spectral resolving power ($E/\Delta E$) of these detectors is limited to about 2.5 at 1 keV by fundamental statistical processes in the gas, and it scales as $E^{1/2}$. Variants exist that can double this resolving power (97, 115, 120), but so far only limited measurements of diffuse emission have been made with them (51, 67, 68).

In addition to information about the spectrum of the incident X rays, the pulse-height distribution provides invaluable discrimination against non-X-ray events. This is particularly important for diffuse background studies, where it is not possible to use the discrete source technique of estimating backgrounds by observing a nearby area of empty sky. Other valuable characteristics of proportional counters are a very low background rate and the ease of scaling to large areas with relatively low weight and cost. A more extensive discussion of their application to soft X-ray observations can be found in (55).

The revolution in sensitivity for discrete source measurements provided by imaging X-ray optics has largely bypassed diffuse background studies. The large focal ratios of X-ray telescopes give them less throughput than mechanically collimated detectors for angular resolutions coarser than a degree or so, and thus far no large telescope/detector combination has been flown that was sufficiently well optimized for extended sources to allow routine diffuse background measurements to be made with higher angular resolution. A few experiments, most notably *SAS 3* (45), have successfully used nonimaging reflectors to improve the angular resolution, but most of the data discussed below were obtained with mechanically collimated proportional counters.

The limited energy resolution of proportional counters becomes particularly serious below 1 keV, and at 0.25 keV the resolving power is down to about unity (although the shape of the pulse-height distribution

continues to provide valuable discrimination against non-X-ray counts). Additional spectral information is generally obtained through the use of atomic absorption-edge filters, either placed in front of the counter or incorporated into its entrance window. The bandpass resulting from these filters has a characteristic shape with a sharp cutoff on the high-energy side and a gradual drop toward low energies. This can be seen in the Wisconsin Be-, B-, and C-band response curves of Figure 3; the figure shows the energy discrimination that can be obtained below 2 keV with conventional proportional counters by using pulse-height discrimination at the higher energies and K-edge filters of beryllium, boron, and carbon at lower energies.

Future instruments will include imaging telescopes with fast optics optimized for energies of ~ 1 keV and below, such as the upcoming ROSAT observatory (125). With appropriate detectors, these will enable observations with greatly improved angular resolution. Bragg spectrometers are awkward for diffuse sources, but the Wisconsin Diffuse X-ray Spectrometer (111) will obtain spectra of the 0.25-keV background with ~ 10-eV resolution when it flies as an attached Space Shuttle payload. Microcalorimeters can have similar or better energy resolution with much higher throughput for a given detector size (89, 134).

MAJOR DATA SETS Several experiments have mapped diffuse soft X-ray emission from a large fraction of the sky: (*a*) A University of Wisconsin

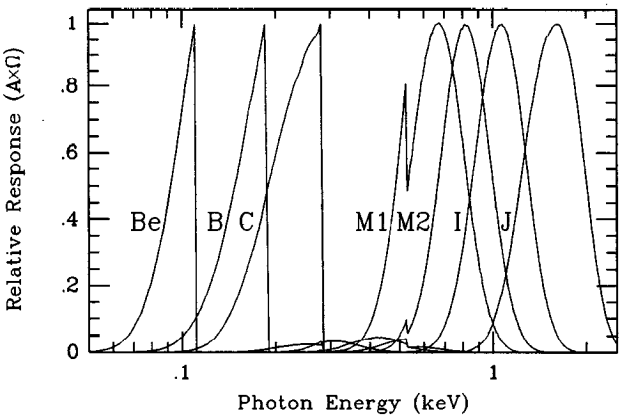

Figure 3 Band response functions obtainable from proportional counters below 2 keV. The M1, M2, I, and J bands are defined primarily by using the pulse-height resolution of the counter. The Be, B, and C bands are defined primarily by the transmission of a filter made of the corresponding element (from 4, 84).

sounding-rocket survey resulted in a set of seven maps covering the energy range 0.12–6 keV with 7° angular resolution and a typical exposure of 500 cm^2 s (84). These data are available on magnetic tape from the National Space Science Data Center or from the authors. (*b*) Marshall & Clark (80) have published a 0.25-keV (C-band) map using data from the *SAS 3* satellite. It has 4.5° resolution and an average exposure of ~ 1000 cm^2 s. (*c*) The Penn State group (G. Garmire, J. A. Nousek, D. N. Burrows & R. L. Fink) has recently completed a set of maps from the A2 LED detectors on *HEAO 1*. Five maps cover the energy range 0.12–3 keV with 3° resolution and typical exposures of ~ 8000 cm^2 s (32). The maps are available from those authors as FITS images. (*d*) The Goddard Space Flight Center X-ray group (E. Boldt et al) is preparing 2–20 keV maps from the *HEAO 1* A2 MED and HED detectors (106) and expects to publish them in 1990. These data are not yet distributed, but they are available at Goddard. Figures 4–7 compare sample maps from (*a*), (*b*), and (*c*) above.

CAVEATS: HOW RELIABLE ARE THE DATA? Extraneous signals are a serious problem for any diffuse background measurement. In principle, contamination levels can be estimated only by evaluating each physical process that is a potential contributor and then finding some way to estimate or limit its magnitude. There clearly can never be a guarantee that you have thought of everything.

The most important sources of non-X-ray contamination are cosmic rays, ultraviolet photons, and electrons in the 2–50 keV energy range that can penetrate thin detector windows. Noncosmic X rays may come from solar X rays scattered in the upper atmosphere, from thermalization of the solar wind, or from an intense flux of low-energy electrons that can produce X rays by bremsstrahlung from the atmosphere or from surfaces in the instrument itself. X-ray observations below 1 keV require thin detector windows and are the most susceptible to all of these effects. Electron contamination is particularly troublesome for satellite experiments, as it varies strongly with orbital position as well as with time. These mechanisms are discussed in detail in (81) and (82). Methods for estimating limits to their contributions are dealt with in (84).

Some general arguments help increase our confidence in the data. The most powerful of these result from multiple observations of the same part of the sky at different times and from different locations. We would expect any source associated with the Earth or the solar system to be variable in time on the many-year scale over which some of these observations have been repeated, and those associated with the upper atmosphere should look different from different altitudes or latitudes. Figures 4 and 5 show the $\sim$160–284 eV (C-band) maps from the Wisconsin and *SAS 3* sky

surveys, respectively. A comparison of these is comforting, since, except for two areas in the Wisconsin survey that had been identified as likely to be contaminated by electrons (84), there is excellent feature-by-feature agreement between them. These maps were made with very different instruments (one had mechanical collimators, the other a reflective concentrator), from different vantage points (one was done from sounding rockets, the other from a satellite), and many years elapsed between the observations for some parts of the sky. A similar comparison can be made for the $\sim$500–$\sim$1100 eV (M-band) maps from the Wisconsin and *HEAO 1* A2 LED surveys shown in Figures 6 and 7, respectively.

The band responses on the various surveys are slightly different, so a source spectrum must be assumed to make absolute flux comparisons. Using a $10^{6.0}$-K thermal emission spectrum that fits the average observed B/C-band rate ratio on the Wisconsin survey, the *SAS 3, HEAO 1*, and Wisconsin C-band average observed rates all agree within 10%. The M-band spectrum is more variable across the sky, but we again take the all-sky average M1/M2-band rate ratio from the Wisconsin survey to fix the temperature of a thermal emission model at $10^{6.5}$ K. With this source spectrum, the *HEAO 1* and Wisconsin M-Band (combined M1 + M2 from the Wisconsin survey) average absolute fluxes fortuitously agree to better than 1%.

These comparisons are encouraging. However, large amounts of data were discarded in each of these surveys owing to internal disagreement of repeated observations or other indications of contamination, so time-variable contamination, usually from electrons, is a common occurrence. It is therefore prudent to regard with considerable caution any feature that has been observed only once. We also point out that while the possibility of an isotropic, time-invariant extraneous contribution seems remote, it cannot be ruled out by repeated observations, and many of the interpretations of the data discussed below would be profoundly affected by the removal of an isotropic component equal in magnitude to the minimum observed intensity.

MAJOR OBSERVATIONAL CHARACTERISTICS AT DIFFERENT ENERGIES For convenience in the following discussion, we divide the soft X-ray region into three energy ranges. These are not entirely arbitrary but are chosen because of evidence that different source mechanisms dominate in each.

2–10 keV Diffuse flux in this energy range comes largely from the extragalactic background. Between 3 and 10 keV, the spectrum can be fit by a $\sim 8E^{-0.4}$ keV (cm^2 s sr keV)$^{-1}$, power law [79, 113, 114; also personal communication of *Ginga* (126) results by Y. Tanaka]. There is some disagreement on the absolute intensity of this spectrum. Many sounding-

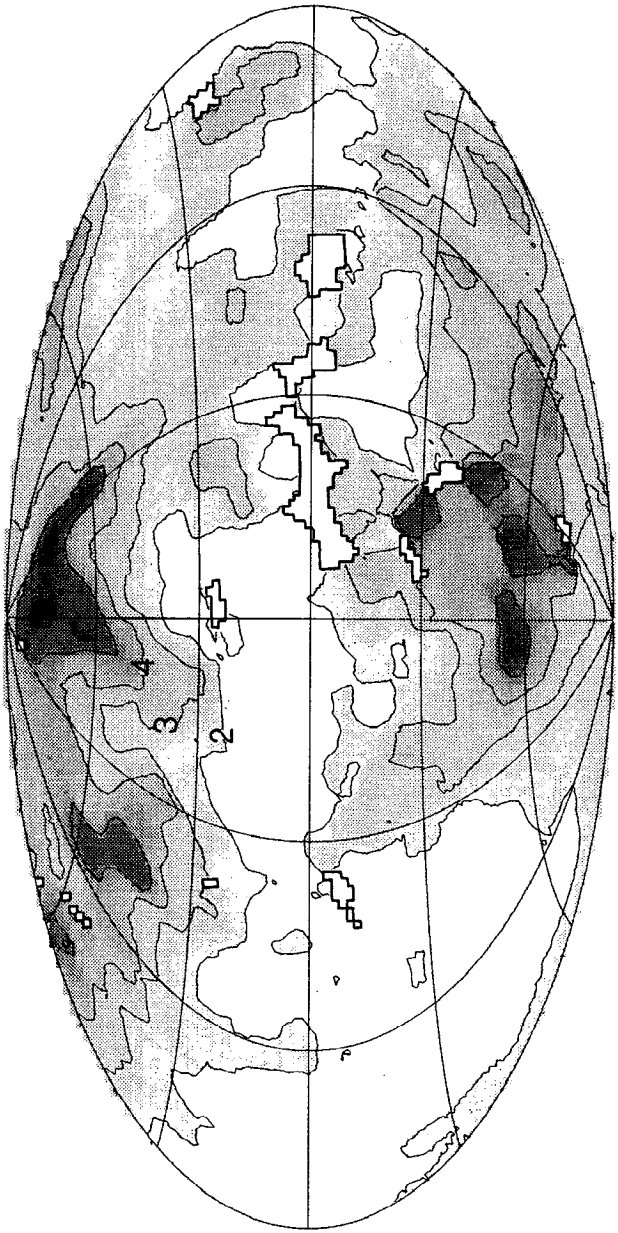

Figure 4 C-band (~ 160–284 eV) map from the Wisconsin sky survey (84). The map is in galactic coordinates, with $l = 0°$ at the center and increasing to the left. The contour unit is 0.001 cm^{-6} pc emission measure for a $10^{6.0}$-K equilibrium plasma with solar abundances (99a) and no interstellar absorption. Bright discrete sources have been removed from the Wisconsin maps.

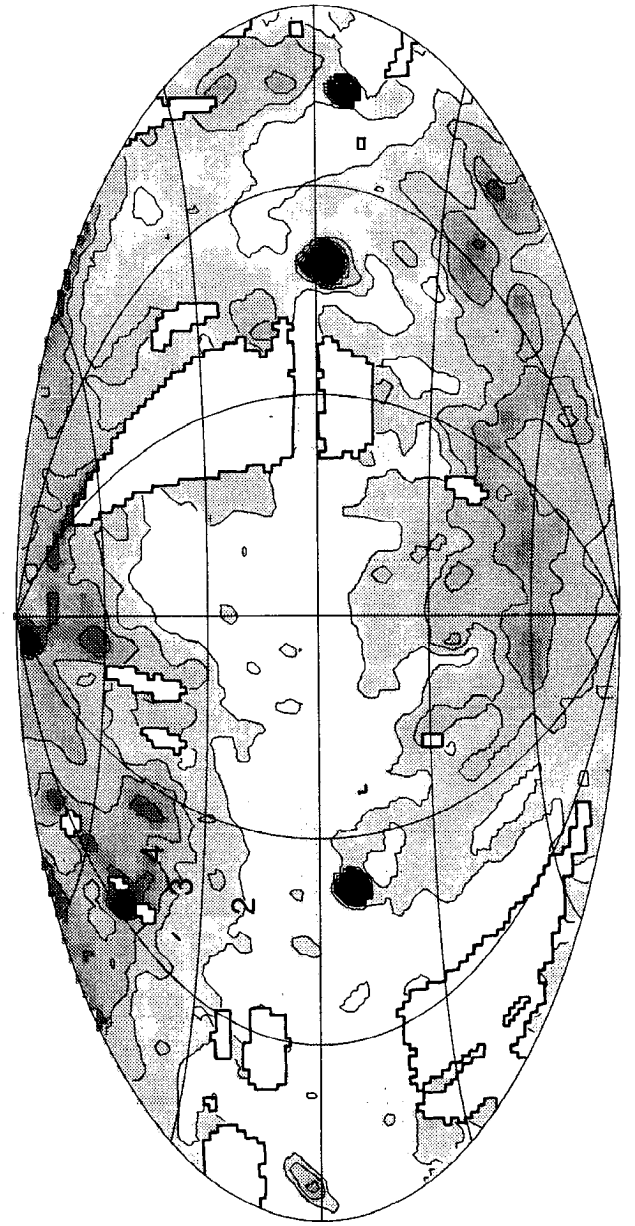

Figure 5 C-band (~130–284 eV) map from the *SAS 3* survey (80). Same projection and contours as in Figure 4.

Figure 6 M-band (~490–~1090 eV) map from the Wisconsin sky survey (84). The map is in galactic coordinates, with $l = 0°$ at the center and increasing to the left. The contour unit is 0.001 cm^{-6} pc emission measure for a $10^{6.5}$-K equilibrium plasma with solar abundances (99a) and no interstellar absorption. Bright discrete sources have been removed from the Wisconsin maps.

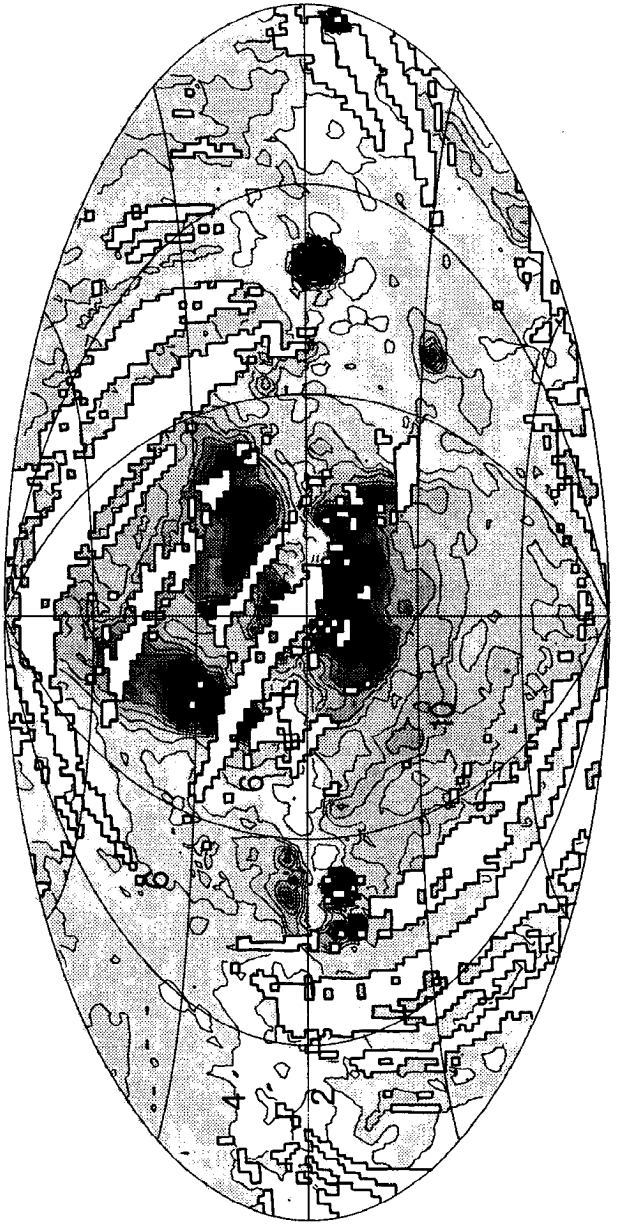

Figure 7 M-band (~480–~960 eV) map from the *HEAO 1* A2 LED survey (32). Same projection and contours as in Figure 6.

rocket experiments report fitting a power law closer to $11E^{-0.4}$ keV (cm^2 s sr keV)$^{-1}$ (13, 26, 33, 48, 94). The experiments giving the higher values in most cases had less sensitivity at the higher energies, and more sensitivity below 3 keV, so the obvious conclusion would be that the spectrum steepens at the low end of the 2–10 keV range. The results are not so easily reconciled, however, as this should also have resulted in a steeper power-law index in the thin-window experiments. The single most precise measurement in the 3–10 keV range seems to the *HEAO 1* A2 MED/HED survey (79), so we provisionally adopt the $8E^{-0.4}$ fit to their data, keeping in mind that the intensity (at least at 2 keV) may be as much as 30% above this spectrum.

This is an important point, since spectra for most of the discrete sources that are supposed to contribute significantly to the extragalactic background have been measured primarily in the 1–3 keV range. On the other hand, a galactic origin for the possible excess flux at 2 keV cannot be ruled out. Below 1 keV, the extragalactic flux is unknown: Here the poorly determined galactic emission could clearly be an important or dominant contributor.

In addition to the isotropic extragalactic flux, two relatively faint galactic emission components have been identified (54, 129, 130, 133). One is a narrow ridge confined to the galactic plane, with a scale height of $\sim$250 pc and a radial extent of $\sim$10 kpc. It has a spectrum that is considerably softer than the extragalactic background, being consistent with thermal plasma emission with kT varying from $\sim$3 to 14 keV in different directions (67, 68). This spectral variation leads to the conclusion that if discrete sources are responsible, their number cannot be so large that variations are averaged out, implying a minimum luminosity of about 10^{33} ergs s^{-1} for the individual sources. The spectrum has been found to show strong emission lines of highly ionized iron, apparently confirming a thermal origin (68). The second emission component has a nominal scale height of several kiloparsecs (54). This component is much fainter but has a similar spectrum that recently has also been found to contain iron lines (67), although these were not seen by *HEAO 1* (54). The similar spectra indicate that both these components may have the same origin. It seems unlikely that either is truly diffuse, but no known class of discrete sources meets all of the requirements (127).

0.5–1 keV The spatial structure in this energy range is dominated by an irregular feature about 110° in diameter located in the general direction of the galactic center (see Figures 6 and 7) whose boundaries coincide roughly with the outline of radio Loop I [3; see also the H I map in the review by Dickey & Lockman (26a) in this volume]. The two brightest parts of the

boundary of the northern half line up very well with the brightest sections of the radio ridge defining Loop I, and there can be little doubt that these are related. The bright knots in the interior appear to be associated with Loop I, but they might also represent emission from hot gas around the galactic center (35). Loop I and its relation to the X-ray emission have been discussed in a number of papers (8, 25, 42, 46, 53, 92). Two other, much smaller features that show up clearly on these maps are the Eridanus-Orion enhancement near 200°, −35° (90, 92, 101) and the Cygnus "super-bubble" at 80°, +5° (20; this feature has been partially removed from Figure 6 along with the Cygnus Loop).

Aside from these features, the spatial distribution is quite smooth, with an intensity that exceeds an extrapolation of the $8E^{-0.4}$ keV (cm^2 s sr keV)$^{-1}$ extragalactic spectrum by more than a factor of 2. The intensity shows almost no variation in going across the galactic plane at most longitudes. This is quite curious, since an extragalactic or halo source should be completely absorbed in the galactic plane, while any source distributed throughout the disk should be much brighter near the plane than at the poles. Figure 8 shows the average latitude dependence of the M1+M2-band (~490–~1090 eV) data, excluding the quadrant $270° < l < 60°$ containing Loop I and a small region containing the Eridanus-Orion feature.

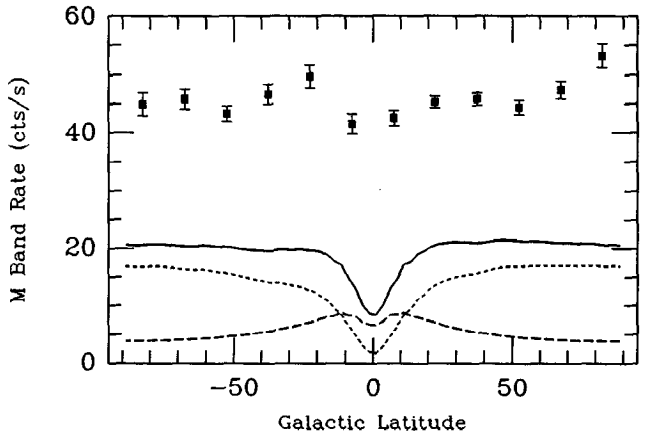

Figure 8 Average M-band (~490–~1090 eV) counting rate as a function of galactic latitude. Longitudes including Loop I ($270° < l < 60°$) have been excluded, as has a small region around the bright feature in Eridanus. The short-dashed line shows the calculated contribution from an assumed $8E^{-0.4}$ keV (cm^2 s sr keV)$^{-1}$ extragalactic source. The long-dashed line is the calculated contribution from dM stars (J. Schmitt & S. Snowden, personal communication). The solid line is the sum of these. Data are from (84).

A few observations of the 0.5–1 keV background have been made with instruments providing better than the usual proportional counter energy resolution. Inoue et al (51, 52) observed regions near the North Galactic Pole and North Polar Spur with a gas scintillation proportional counter with about 200-eV FWHM resolution at 600 eV. They report strong evidence for emission lines of O VII and O VIII. Schnopper et al (112) and Rocchia et al (103) observed essentially the same regions with a silicon solid-state detector ($\sim$150-eV FWHM resolution), and their data clearly show line emission due to O VII and good evidence for several other lines. This is a direct demonstration of the existence of an interstellar plasma in the 1–4 $\times$ 10^6 K temperature range in these directions, and these experiments represent the first step toward obtaining the wealth of information available in higher spectral resolution observations.

70–284 eV Proportional counters offer little useful energy resolution in this range, but K-edge filters allow it to be divided into three reasonably distinct bands, which we refer to as the Be, B, and C bands after the elements employed in the filters. Figure 3 shows the response of the Wisconsin version of these bands. Other thicknesses for the filters will change the low-energy cutoffs somewhat.

The spatial distribution at these energies is quite different from that in the M band, but all three of the low-energy bands appear quite similar to each other. As can be seen in Figures 4 and 5, the intensity is relatively low and uniform in the galactic plane and increases by a factor of 2 to 3 at high latitudes. There is a good deal of structure. The X-ray intensity below 284 eV shows a striking anticorrelation with the total column density of interstellar atomic hydrogen ($N_{\mathrm{H\,I}}$). The anticorrelation between $N_{\mathrm{H\,I}}$ and the Wisconsin C-band intensity is shown in Figure 9 and results from structure in longitude as well as from the general latitude variations. This is qualitatively the signature expected for an absorbed extragalactic flux, but it is difficult to fit quantitatively with an acceptable model. The effective absorption cross section must be much reduced from the normal atomic cross sections. In addition, attempts to find correlations with specific absorbing features have had mixed results. Some H I features that should be optically thick produce no X-ray variation at all, whereas others show clearly correlated reductions in the X-ray flux, although seldom with the expected quantitative behavior or energy dependence (16). This is in sharp contrast to the case for interstellar absorption of soft X rays from supernova remnants at known distances, which is found to be in good agreement with atomic cross sections (102, 107). As discussed in Section 5 below, it now seems probable that most, if not all, of the observed X rays below 284 eV come from closer than at least 90% of the interstellar gas.

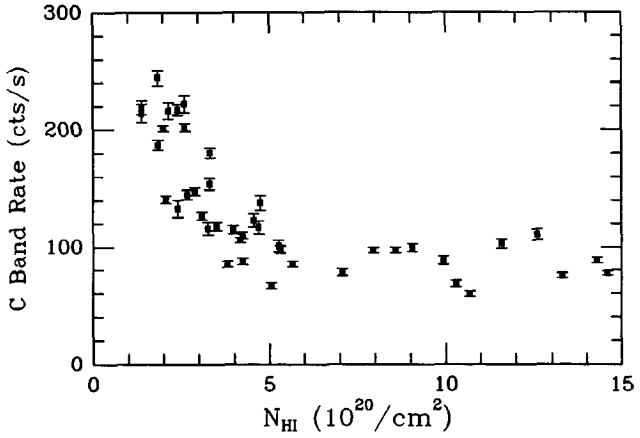

Figure 9 C band (~160–284 eV) rate from the Wisconsin survey (84) plotted against total H I column density (20a). Excluded regions of the sky are the same as in Figure 8. Plotted values are averages over 22.5° in galactic latitude by 30° in longitude. This X ray vs. H I anticorrelation has the qualitative appearance of an absorbed distant source, but this probably is not the case. See text.

The B band map (84) appears quite similar to the C-band map in Figure 4, although the ratio of counting rates varies significantly from one part of the sky to another. The B/C count-rate ratio is plotted against total H I column density in Figure 10, which shows that these variations have only a very slight correlation with $N_{H\,I}$. If one assumes that the X rays are produced by thermal emission from a collisional equilibrium plasma with solar abundances, the models of Raymond & Smith (99a; see also 98) require a temperature range of only 0.9–1.2 $\times$ 10^6 K to produce the observed range of ratios in the absence of significant interstellar absorption.

Sounding-rocket observations below the beryllium K-edge at 111 eV have sampled seventeen 15° $\times$ 15° fields (~10% of the sky) over a wide range of galactic latitudes and longitudes on two flights (4, 63). For almost all of these fields, the ratio of Be-band to B-band counting rates is the same to within the ~15% statistical precision of the individual measurements. (Figure 11 shows the as-yet unpublished data from the second flight.) This is considerably more constant than the B/C ratio: a surprising result, because the interstellar absorption cross sections for the C and B bands differ by only a factor of 2, whereas the Be-band effective cross section is about 6 times larger than that for the B band. Since an H I column density of only 1 $\times$ 10^{19} cm^{-2} (about 5% of the average high-latitude total) represents one optical depth for the Be band, very small amounts of

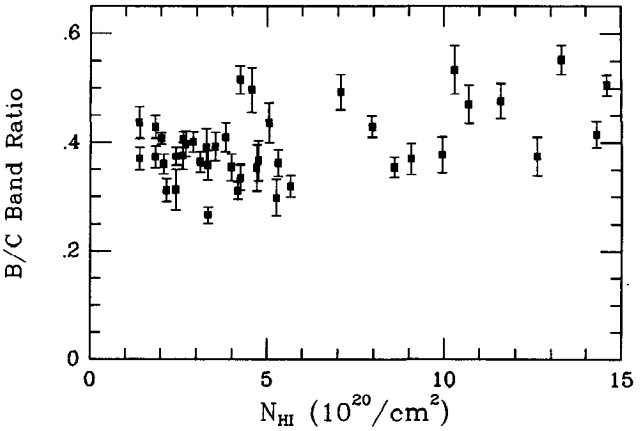

Figure 10 Ratio of counting rates in the B and C bands plotted against total H I column density (20a). The variations in this ratio are spatially very coherent: All points with B/C > 0.4 are contiguous in a region roughly centered on $l = 160°$, $b = +15°$. Excluded regions are the same as in Figure 8.

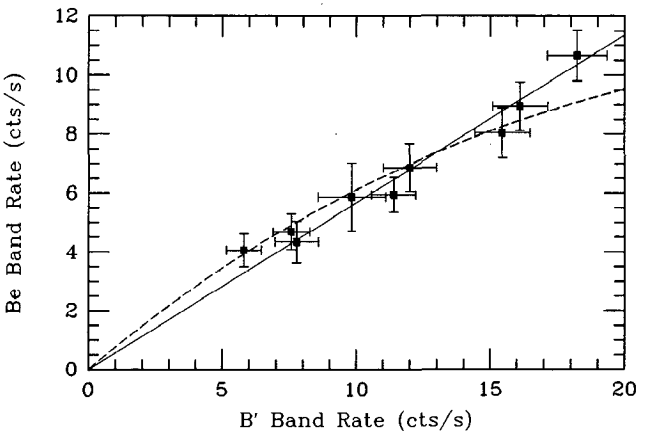

Figure 11 Be-band (~70–111 eV) vs. B′-band (~100–188 eV) rates for nine 15° × 15° fields widely distributed across the sky (62). The straight line shows the relation expected if there is no intermixed absorbing gas. The dashed curve shows the relation expected for uniformly intermixed absorbing material with a total column density of $\sim 1.4 \times 10^{19}$ cm^{-2} to the edge of the X-ray-emitting gas for the brightest point. This is a 2σ upper limit to what is allowed by the data.

foreground absorption should produce large changes in the Be/B ratio. The observed ratio is reproduced by the 1984 Raymond & Smith model for a 10^6-K plasma with no absorption, and the predicted ratio is almost independent of temperature over the small interval required to produce the observed range of B/C ratios (4). One should be cautious about regarding this as more than a happy coincidence, however, since the simple assumptions of this plasma emission model may be a poor approximation to reality.

A recent, partially analyzed third rocket flight observed an additional eight fields in the Be band, including some targets where the Be/B ratio might be expected to be different owing to the presence of a nearby absorbing cloud or a more distant source that should contribute mostly to the B band. The five random fields showed the same relation to the B band as the previous flights, while the other three were 25–50% lower (B. Edwards, personal communication). Analysis is proceeding to see if these results are consistent with interstellar absorption or with emission from much higher temperatures.

A grating spectrometer experiment has been flown on a rocket by the Berkeley group in a pioneering effort to obtain a high-resolution spectrum of the diffuse background in the 20–150 eV energy range (73). This first attempt produced marginal detections for two soft X-ray lines at 70 and 125 eV and demonstrates the promise of this type of observation.

Overview Figure 12 shows the total soft X-ray diffuse background spectrum from (84). The plotted points are the all-sky average fluxes for each of the energy bands, excluding the quadrant containing Loop I. The upper end of the vertical "error bar" is the average for $|b| > 60°$, and the lower end is the average for $|b| < 20°$. This figure should be interpreted with some caution. First, a cursory examination of the maps shows that this spectrum is a composite of independent components that dominate at different energies. Second, the differential fluxes have been plotted assuming continuous spectra, whereas thermal emission lines probably dominate for $E<1$ keV. [Sufficient information for determining the corresponding thermal emission measures can be found in (84).] The horizontal error bars show the shift in the appropriate effective energy for the point in going from an assumed $E^{-0.5}$ to an $E^{-1.5}$ spectrum.

4. *Models of the 0.5–1 keV Emission*

The M-band sky consists of a few bright extended features superimposed on an otherwise nearly isotropic background. The most prominent features are radio Loop I, with the associated North Polar Spur, the Eridanus enhancement, and the Cygnus superbubble. Each is associated with struc-

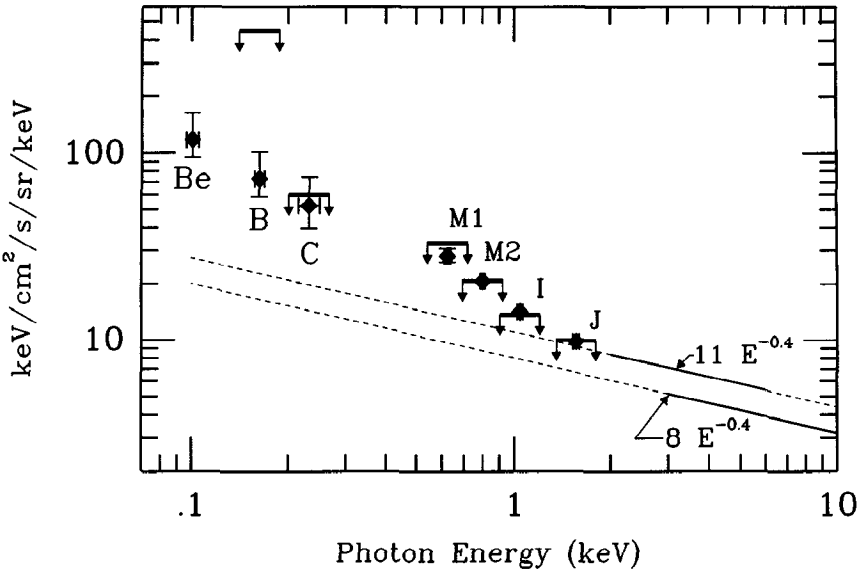

Figure 12 Average observed diffuse background intensity vs. energy. The plotted points are the all-sky averages (with the same exclusions as in Figure 8). The upper "error bar" is the average for $|b| > 60°$, while the lower "error bar" is for $|b| < 20°$. Be-band points assume that the unobserved part of the sky also tracks the B band. The intensities are plotted for an assumed E^{-1} power-law spectrum. The correct effective energy for each point is sensitive to the assumed spectral index: The horizontal error bars show the effect of a ± 0.5 change. The heavy bars represent the best upper limits that can be placed at each energy for the flux incident on the Galaxy from an extragalactic or halo source.

tures observed in the same directions at 21 cm or other wavelengths and has been modeled as a large cavity in the ISM, formed either by stellar winds from young associations or by a series of supernovae, and then heated at a large diameter by a subsequent supernova (8, 17, 20, 25, 42, 43, 46, 53, 91, 92, 101). These features are seen also in the C band where interstellar absorption permits.

The remaining flux mirrors none of the strong latitude and longitude dependence of the 0.25-keV background. Equilibrium thermal emission at 1.0×10^6 K that would provide all of the 0.25-keV flux in fact would contribute only a few percent to the M bands. It is possible to concoct emission mechanisms that produce the entire 0.25–1 keV spectrum in a particular direction (1, 28, 50), but given the disparate spatial structure above and below 0.5 keV, there is little motivation for doing so.

The minimal latitude dependence shown in Figure 8 is a strong observational constraint. The intermediate interstellar mean free path (800 pc

at 0.78 keV) implies a strong latitude dependence for anything but a very local source. Two contributors that should exist at some level are an extrapolation of the observed extragalactic spectrum and the integrated contribution of dM stars (19, 47, 104; J. Schmitt & S. Snowden, private communication). Estimates for both of these are shown in Figure 8. Their combined latitude dependence is consistent with the observations, but an additional, nearly isotropic component is required for $\sim 55\%$ of the flux. So far, we know of no proposal for a local isotropic M-band source compatible with an anisotropic local 0.25-keV source. Several published attempts to model the M-band flux either fail to predict the observed latitude dependence near the plane (64, 92) or fail to reproduce the observed longitudinal isotropy (14, 109).

5. *Models of the 70–284 eV Emission*

Essential features of the data that must be addressed are (*a*) that the soft X-ray intensity is lowest in the galactic plane and increases by a factor of 2–3 at high latitudes; (*b*) that the intensity varies by up to a factor of 3 with longitude at some latitudes; (*c*) that the intensity is strongly but imperfectly anticorrelated with the column densities of atomic hydrogen measured at 21 cm; (*d*) that this anticorrelation exhibits no systematic energy dependence; and (*e*) that the sky maps in the B and C bands are quite similar to one another, with available Be-band observations suggesting a spatial distribution nearly identical to that of the B band.

In this section we describe three simple pictures that have been suggested for interpreting the Be-, B-, and C-band diffuse background. Each picture is clearly an oversimplification and only approximates the observations, but each has the virtue of a manageable number of free parameters. Following our discussion of the simple pictures, we briefly touch on more complete models of the ISM that attempt to include mechanisms for the formation and maintenance of their density and temperature structure in a self-consistent way.

ABSORBED EXTRAGALACTIC OR CORONAL EMISSION The observation that the soft X-ray intensity is highest at high galactic latitudes and lowest in the galactic plane leads easily to the suggestion of an extragalactic or halo origin for the soft X rays beyond the neutral gas of the Galaxy (10, 12, 49, 80, 118). The existence of a dominant extragalactic component is well established for the higher energy diffuse background, while support for an X-ray-emitting halo comes from the suggestion that a 3×10^6-K halo would provide enough pressure to confine high-latitude neutral clouds (122). In these pictures, intensity variations of the soft X rays are caused by absorption of this extragalactic flux by the intervening column of

interstellar neutral gas, which is observed to be small at high galactic latitudes and large in the galactic plane. The opacity of this column is so high at low latitudes for X-ray energies below 1 keV that models using primarily an extragalactic or coronal component must include an additional local component to provide the flux observed in the galactic plane.

The strength of such a picture is that it produces a negative correlation of soft X-ray intensity with $N_{\mathrm{H\,I}}$, but its major weaknesses are that the predicted falloff of soft X-ray intensity with increasing $N_{\mathrm{H\,I}}$ is much steeper than is observed, and that an energy dependence of the falloff is predicted where none is seen. In addition, such a picture explains neither the large scatter in the correlation nor the lack of correlation toward some galactic $N_{\mathrm{H\,I}}$ features. Clumping of the interstellar gas, typically into clouds of thickness several times 10^{20} H I cm^{-2}, could reduce the predicted falloff of X-ray intensity with increasing $N_{\mathrm{H\,I}}$ to match that observed and eliminate the energy dependence of the falloff as well (9, 12), but 21-cm and other interstellar studies over all conceivably relevant angular scales have shown that the necessary clumping is not present in the galactic H I (27, 56, 57).

EMISSION FROM A LOCAL CAVITY ("DISPLACEMENT" MODEL) In this picture, the soft X-ray background originates entirely from a local emission region occupying an anisotropic H I cavity of suitable size and shape in which the Sun is also located (21, 44, 69, 108, 110, 124). Variations in the observed X-ray intensity are due to variations in the extent of the emission volume along the line of sight. In directions with a larger X-ray intensity, the emitting region extends farther along the line of sight, "displacing" more of the neutral material. The negative correlation between soft X rays and $N_{\mathrm{H\,I}}$ that is generated by the competition for space between the hot X-ray-emitting component and the cooler absorbing material fits the observations at least as well as the absorbed extragalactic or coronal emission models. It also results in a reasonable value for the interstellar pressure, which is effectively the only free parameter in such a model when it is fit to the observed H I distribution (121). The required hot-gas cavity is also more or less consistent with the local H I–deficient region crudely outlined by interstellar ultraviolet absorption studies (95). Since the magnitude of the X-ray vs. $N_{\mathrm{H\,I}}$ correlation is unrelated to atomic absorption cross sections in this displacement picture, it naturally should be independent of X-ray energy. Scatter in the correlation is expected because any structure in the H I outside the cavity would be unrelated to X-ray emission inside the cavity.

The emission is assumed to arise from a hot plasma that occupies the local cavity but does not necessarily fill it. This plasma has been modeled

as an expanding adiabatic blast wave (1, 22, 28, 29) or as the interior of an older superbubble (50). Cox & Reynolds (23) have recently reviewed the local ISM, the local cavity, and its X-ray emission. The displacement picture seems to account for all of the observed behavior in the three soft X-ray bands and is the simplest of the simple pictures in that it involves the fewest free parameters.

Although this picture requires no absorption at all for a good fit, it is known from optical and UV observations that small amounts of cooler material exist within the local cavity (see ref. 23 for a summary), and solar Lα backscattering measurements show that the Sun is itself embedded in a low-density cloud of a few parsecs extent in which $n_H \sim 0.1$–0.2 cm^{-3}. Juda (62; Juda et al, in preparation) has examined the effects of optically thin absorbing clouds uniformly intermixed with the hot gas in the cavity. If there is more than a very small amount of included H I, the predicted intensity no longer increases proportionally to path length within the hot cavity but instead tends to saturate as the optical depth approaches unity at each energy. This introduces a curvature to the expected Be-band vs. B-band relation, as shown in Figure 11. Observational limits to this curvature place a 2σ upper limit of $\sim 7 \times 10^{18}$ H I cm^{-2} on the total column density along an average path to the edge of the emitting region (62). For the best-fit cavity with $\langle R \rangle = 100$ pc, this gives $\langle n_{H\,I} \rangle < 0.02$ cm^{-3} and allows a filling factor of up to 25% for cloudlets similar to the one surrounding the Sun.

ABSORBERS INTERMIXED WITH EMISSION In this picture, the X-ray-emitting material is intermixed with the interstellar absorbing material (15, 18, 23, 26, 34, 41, 58, 65, 76). A strength of this model is that intermixture reduces the predicted magnitude of absorption, but the models so far have been unable to reproduce all of the major features of the data.

Jakobsen & Kahn (58) have developed a framework for exploring the effects of an embedded cloud geometry on the very soft X-ray background. They include explicitly in their analysis the effects of absorbing clouds randomly interspersed within the emitting medium. In this statistical idealization, they find that the properties of the background depend on two parameters: R, the ratio of the scale height of the absorbing clouds to that of the X-ray emission; and η, a parameter that describes the reduction of the effective cross section of the absorbing component caused by its being clumped into clouds. ($\eta = 1$ corresponds to no clumping; $\eta = 0$ corresponds to infinite clumping.) Jakobson & Kahn find that these parameters are not severely constrained by the observed smoothness of the background nor by the shape of the anticorrelation of soft X-ray intensity versus $N_{H\,I}$, but the galactic latitude dependence of the data is a significant

constraint. The increase in soft X-ray brightness at high galactic latitudes would require values of $\eta \sim 0.5$ and $R \sim 0.1$, where most of the emission is behind most of the (highly clumped) absorbing gas. This model is essentially the same as the absorbed coronal model discussed above, including its requirement for more extreme clumping of the absorbing material than seems allowed by observations.

Since one is restricted to $\eta \sim 1$ by the observed lack of clumping, then R is also required to be about unity to reproduce the observed constancy of the B/C and Be/B count-rate ratios (65). This works because with equal scale heights for emission and absorption, the source function $S_\nu = \Lambda_\nu n_e^2/4\pi\sigma_\nu n_H$ is constant along a line of sight, and the observed intensity I_ν saturates at this value. (Here $\Lambda_\nu n_e^2$ is the volume emissivity for electron density n_e, and σ_ν is the frequency-dependent cross section per hydrogen atom.) This is not really a "model" in the usual sense of the word, since it predicts equal X-ray intensity in all directions. An obvious implication here is that one could introduce intensity variations and get an energy-independent anticorrelation of I_x with N_H by making n_H different in different directions. A little reflection reveals that there is no geometrically reasonable way of doing this, since n_H must remain approximately constant along the length of each line of sight. Instead, the requirements of homogeneity and uniform statistical properties must be relaxed, and large-scale structures introduced. The above authors are working on models of this sort; the challenge is to create one in which the observable part of it is significantly different from the local cavity model described above.

In one example of such a modification, Burrows (15) fit the Wisconsin C-, B-, and Be-band data to an embedded cloud model with the addition of a local unabsorbed component. He found that the model with appreciably intermixed emission and absorption could be rejected based on the χ^2 residual, but the formal application of such statistics to simple models that are known to be incomplete descriptions of reality is questionable.

MORE COMPREHENSIVE MODELS Ultimately, we would like a successful model of the nature and origin of the soft X-ray background to be part of a more comprehensive model of the ISM that includes mechanisms for producing and maintaining its structure. Cox & Reynolds (23) have reviewed models of the local ISM, paying particular attention to the constraints afforded by the soft X-ray observations, and they conclude that the local ISM is not typical of the general ISM. Two competing pictures emerge from their discussion: that of the local ISM as an older ($\sim 10^7$ yr), quiescent, pressure-confined hot X-ray-emitting bubble (24, 50); and that of the local ISM as a younger ($\sim 10^5$ yr), active, hot X-ray-emitting

supernova remnant (1, 22, 29). Although they acknowledge that the former picture may prove untenable if cloud evaporation provides significant cooling (11, 86), in the absence of evidence for the necessary clouds, they tentatively adopt the quiescent bubble scenario for the local ISM.

In their general ISM model, McKee & Ostriker (86) find a pervasive hot component in a self-consistent steady state where supernova heating is balanced by cloud evaporation, but its mean temperature is too low ($\sim 4 \times 10^5$ K) to produce the observed X rays. The local cavity seems deficient in evaporating clouds, however, which would give it a longer than average lifetime at its elevated temperature.

An elaborate picture of the local ISM has been assembled by Bochkarev (6), who incorporated extensive radio, IR, optical, UV, and X-ray observations of the solar neighborhood into a model with the Sun located near the edge of a giant cavern in the ISM centered on the Sco-Cen OB association. In this model, the X-ray background is produced by shock fronts from the OB association's stellar winds interacting with the cavern walls and the boundary of the small cloud in which the Sun is embedded.

6. *Limits on the Extragalactic Flux*

Below 0.25 keV it now seems likely that very little of the observed flux can come from outside the Galaxy. However, in placing the complementary upper limit on an extragalactic component, one must correct for the opacity of interstellar gas along a line of sight out of the Galaxy. At these energies, the opacity is high even near the galactic poles, and the correction factor is large.

The best limit for the C-band range comes from limits on spatial variation in the observed flux on and near the Small Magellanic Cloud (SMC; 83, 85). The analysis in (85) used an overly conservative criterion for placing confidence limits on parameter values, extending the allowed parameter range to the point where the absolute $P(\chi^2)$ for the model becomes small. Applying the now-standard criteria of Lampton et al (74) to the same χ^2 residuals results in somewhat lower limits for an extragalactic flux at 0.25 keV than were originally reported in (85): The 95% confidence upper limits are 30 keV $(\text{cm}^2\ \text{s sr keV})^{-1}$ for a flux originating beyond the SMC, or 38 keV $(\text{cm}^2\ \text{s sr keV})^{-1}$ for X rays originating closer than the SMC but beyond all of the galactic H I, as for emission from an extended galactic halo. These limits are respectively 2.1 and 2.7 times an extrapolation of the $8E^{-0.4}$ keV $(\text{cm}^2\ \text{s sr keV})^{-1}$ extragalactic spectrum observed above 3 keV.

It has recently been recognized that there is an ionized component of the ISM with a scale height of ~ 1 kpc and a total column density averaging $\sim 1 \times 10^{20} \csc(b)\ \text{cm}^{-2}$ (100). A high-z pulsar fortuitously located directly

in front of the SMC has a dispersion measure corresponding to $N_{\rm H\,II} = 7.2 \times 10^{19}$ cm^{-2} (77a). The presumably neutral helium associated with this H II provides about 0.4 optical depth in the C band, since hydrogen normally is responsible for only 25% of the total absorption (88). This ionized component was not included in the previous analyses, so the above limits should be increased by about a factor of 1.5. The resulting extragalactic upper limits are comparable to the total observed intensity, but after absorption they can account for at most 13% of it in the direction of the SMC. Limits obtained using the Large Magellanic Cloud (LMC; 77) and M31 (78) also require most of the observed flux to be galactic but do not as effectively constrain the extragalactic flux owing to the high interstellar opacity in these directions.

The Wisconsin group also reports a similar limit based on lack of absorption by galactic H I in two other regions of the sky (16). This limit from the simultaneous B- and C-band analysis took advantage of an implicit (and unintended) assumption that the observed contribution of any extragalactic component would be the same for both bands, which is unreasonable. The weaker limits they obtained using the C band alone are valid (but should be corrected for absorption by the high-z H II).

It should be possible to improve these existing 0.25-keV limits by about a factor of 7 (to below a power-law extrapolation of the extragalactic spectrum) with high-angular-resolution observations of compact H I features in regions where the total absorption is particularly low. The ROSAT X-ray telescope is well-suited for such observations.

In the 0.5–1 keV range, it is not possible to use large-scale interstellar absorption to place limits on the extragalactic flux in a way that is independent of the rather unsatisfactory models for galactic emission at these energies. The best that can presently be done is to take the lowest observed intensity, far enough away from the galactic plane such that absorption is negligible, to be an upper limit to the extragalactic contribution. This limit goes from about 3 times the $8E^{-0.4}$ keV (cm^2 s sr keV)$^{-1}$ extrapolation at 0.5 keV to 2 times this extrapolation at 0.8 keV. Again it should be possible to improve these limits considerably with high-resolution observations of compact absorbing features. In this case, however, features with adequate optical depth will probably contain molecular material, which makes determination of the expected absorption more difficult and uncertain. If the local emission is entirely thermal (and therefore 99% in lines), it may also be possible to use high spectral resolution to look between the lines for an excess continuum due to an extragalactic component.

As discussed in Section 3 above, the total observed intensity in the 1–3 keV range is uncertain but may be about 30% above a simple bremsstrahlung or power-law fit to the uncontaminated extragalactic flux above

3 keV. If it is, this additional flux could be due either to a steepening of the extragalactic spectrum or to a galactic contribution. This creates an awkward situation for attempts to determine the contribution of active galactic nuclei (AGNs) to the extragalactic background, since their spectra are currently best determined in this energy range where the diffuse background spectrum is uncertain.

Galactic emission in the 3–10 keV range is quite faint away from the plane and almost certainly makes a negligible contribution to the extragalactic flux at high latitudes. However, structure in the large-scale-height component of the emission serves to confuse searches for the Compton-Getting effect in the extragalactic background, which should otherwise be marginally detectable with current data (K. Jahoda, private communication; 7, 117).

The best current upper limits to the extragalactic flux below 1 keV are shown in Figure 12. These include corrections for the opacity of galactic H I and the high-z H II layer discussed above. Even these crude upper limits provide useful constraints on contributions to the extragalactic background by AGNs with soft spectra (30).

7. *Summary*

Galactic diffuse X-ray emission goes from being a negligible contributor to the extragalactic background at 10 keV to completely dominating it at 0.25 keV and below. Several quite different sources of galactic emission are important at different energies.

In the 3–10 keV range, galactic emission is confined to a thin disk in the galactic plane and a much fainter thick disk. These have similar thermal spectra showing strong emission lines of iron. It is doubtful that either of these represents truly diffuse emission; both are more likely due to a population of discrete sources, although no known class of sources seems to have the right characteristics.

From about 1 to 3 keV, the observed diffuse flux is probably mostly extragalactic, but may be 25–30% higher than an extrapolation of the 3–10 keV spectrum. This excess could be either galactic or extragalactic, with some consequences for models of AGN contributions to the background.

The 0.5–1 keV range is probably the most poorly understood part of the diffuse X-ray background. A power-law extrapolation of the extragalactic spectrum above 3 keV would account for about 35% of the flux observed at latitudes above 20°, where interstellar absorption is negligible. Discrete sources can contribute at most another $\sim$15% of the high-latitude flux. There are a small number of identifiable bright features, such as Loop I and the Cygnus and Eridanus "superbubbles," that appear to be pockets of hot gas near 3×10^6 K with radii of 100 pc or so. At this temperature

and higher, we should be able to see all such features out to at least 1 kpc, and their filling factor appears to be less than 10%. Aside from these isolated features, the background in this energy range is quite smooth, showing only a slight tendency to decrease in the galactic plane (Figure 8).

The most straightforward way to account for this distribution is to postulate a very local isotropic source that provides about two thirds of the observed M-band photons. The expected contributions from an $8E^{-0.4}$ keV (cm^2 s sr keV)$^{-1}$ extragalactic spectrum and dM stars then fill in the remainder and give a reasonable fit to the average latitude dependence. An alternative is to assume that the extragalactic spectrum steepens below 2 keV to provide most of the observed M-band flux at high latitudes, or, equivalently, that there is a large-scale-height halo. A second source distribution is then needed in the galactic disk, whose scale height and intensity must be carefully adjusted to fill in for the interstellar absorption of the extragalactic component. In any of these cases, there must be some as-yet unidentified galactic component. High-resolution spectra could provide important clues for the physical origin of this flux, while high-spatial-resolution observations of potential absorbing features would place limits on its location.

The observed 70–284 eV background is almost entirely galactic. More than half of it must originate within a few hundred parsecs of the Sun; quite possibly all of it does. It is most easily (but not uniquely) explained as thermal emission from 10^6-K gas filling an irregular cavity around the Sun. The required cavity is consistent with other observations of a low-density cavity in the local ISM, although there are directions in which the X-ray emission would have to end well before a dense wall is encountered. No absorption within the emitting region is required by the X-ray data, but the small amounts of neutral material found by other observations can be accommodated.

Models in which a substantial fraction of the observed 70–284 eV flux comes from beyond all of the neutral hydrogen seem to be ruled out by stringent radio and optical limits on the clumping of the intervening material. Work is currently being done on the more general intermediate case, where hot gas is intermixed with the absorbing material, but it remains to be seen whether this can result in viable models that distribute the observed emission substantially differently from the simple cavity model. Any guidance that such models could give toward obtaining observational evidence for or against more widespread hot gas would be valuable.

In any case, the Sun *is* in an H I hole—i.e. the average density for ~ 100 pc in most directions, and much farther in some, is much less than the galactic average of 1 cm^{-3}. A similar path length of gas at 10^6 K will provide the observed 0.25-keV X-ray flux at a reasonable pressure ($\sim 10^4$

cm^{-3} K; 23). It seems logical enough to put the two together. The result can be interpreted in three ways: (*a*) The Sun is in an unusual location; (*b*) most of the H I in the Galaxy is organized into sheets on scales of a few hundred parsecs, with hot gas filling a large fraction of volume between; or (*c*) a situation in between (*a*) and (*b*) is the case, where we have a "normal" intermixture of clouds and intercloud medium, with some modest filling factor of hot bubbles. It is indicative of our current state of understanding of the global organization of the ISM that we cannot discriminate among these disparate pictures (72).

There is considerable reason to hope for an improvement in our understanding of galactic soft X-ray emission in the not-too-distant future. The German X-ray telescope on ROSAT is nearly an optimum design for studying diffuse emission at high angular resolution. This should allow detailed absorption studies to determine the location of the X-ray emission. Its all-sky survey program should provide maps of the global distribution in the 0.1–2 keV region with more than an order-of-magnitude improvement over existing data in both angular resolution and statistical precision. Observations of other galaxies will allow at least upper limits to be placed on the total amounts of 10^6-K gas in the disks of galaxies similar to our own. Measurements with Bragg spectrometers and microcalorimeter detectors will resolve the emission-line spectra of thermal sources, providing detailed information on the physical conditions in the source plasmas as well as indications of the time since heating. Observations of the individual emission lines should also make it possible to unambiguously distinguish galactic thermal emission from a truly extragalactic source.

ACKNOWLEDGMENTS

We thank D. P. Cox, W. L. Kraushaar, F. J. Lockman, and R. J. Reynolds for helpful discussions and critical readings of the manuscript; the Penn State group for permission to use their all-sky maps; J. J. Bloch for preparing Figure 2; and B. Edwards and M. Juda for their unpublished results. This work was supported in part by NASA grant NAG 5-629.

Literature Cited

1. Arnaud, M., Rothenflug, R. 1986. *Adv. Space Res.* 6: 119–28
2. Baity, W. A., Peterson, L. E., eds. 1979. *X-Ray Astronomy*. Oxford: Pergamon. 558 pp.
3. Berkhuijsen, E. M., Haslam, C. G. T., Salter, C. J. 1971. *Astron. Astrophys.* 14: 252–62
4. Bloch, J. J., Jahoda, K., Juda, M., McCammon, D., Sanders, W. T., Snowden, S. L. 1986. *Ap. J. Lett.* 308: L59–62
5. Bloemen, H. 1989. *Annu. Rev. Astron. Astrophys.* 27: 469–516
6. Bochkarev, N. G. 1987. *Astrophys. Space Sci.* 138: 229–302
7. Boldt, E. A. 1977. *Phys. Rep.* 146(4): 215–57
8. Borken, R. J., Iwan, D. C. 1977. *Ap. J.* 218: 511–20

9. Bowyer, C. S., Field, G. B. 1969. *Nature* 223: 573–75
10. Bowyer, C. S., Field, G. B., Mack, J. E. 1968. *Nature* 217: 32–34
11. Boehringer, H., Hartquist, T. W. 1987. *MNRAS* 228: 915–31
12. Bunner, A. N., Coleman, P. L., Kraushaar, W. L., McCammon, D., Palmieri, T. M., et al. 1969. *Nature* 223: 1222–26
13. Bunner, A. N., Coleman, P. L., Kraushaar, W. L., McCammon, D., Williamson, F. O. 1973. *Ap. J.* 179: 781–88
14. Burrows, D. N. 1982. PhD thesis. Univ. Wisc., Madison. 460 pp.
15. Burrows, D. N. 1989. *Ap. J.* 340: 775–85
16. Burrows, D. N., McCammon, D., Sanders, W. T., Kraushaar, W. L. 1984. *Ap. J.* 287: 208–18
17. Burrows, D. N., Nousek, J. A., Truax, R. J., Garmire, G. P., Singh, K. P. 1985. *Bull. Am. Astron. Soc.* 17: 883 (Abstr.)
18. Burstein, P., Borken, R. J., Kraushaar, W. L., Sanders, W. T. 1977. *Ap. J.* 213: 405–20
19. Caillault, J.-P., Helfand, D. J., Nousek, J. A., Takalo, L. O. 1986. *Ap. J.* 304: 318–25
20. Cash, W., Charles, P., Bowyer, S., Walter, F., Garmire, G., Riegler, G. 1980. *Ap. J. Lett.* 238: L71–76
20a. Cleary, M. N., Heiles, C., Haslam, C. G. T. 1979. *Astron. Astrophys. Suppl.* 36: 95–127
21. Cox, D. P. 1977. In *Topics in Interstellar Matter*, ed. H. van Woerden, pp. 17–25. Dordrecht: Reidel. 295 pp.
22. Cox, D. P., Anderson, P. A. 1982. *Ap. J.* 253: 268–89
23. Cox, D. P., Reynolds, R. J. 1987. *Annu. Rev. Astron. Astrophys.* 25: 303–44
24. Cox, D. P., Snowden, S. L. 1986. *Adv. Space Res.* 6(2): 97–107
25. Davelaar, J., Bleeker, J. A. M., Deerenberg, A. J. M. 1980. *Astron. Astrophys.* 92: 231–37
26. Davidsen, A., Shulman, S., Fritz, G., Meekins, J. F., Henry, R. C., Friedman, H. 1972. *Ap. J.* 177: 629–42
26a. Dickey, J. M., Lockman, F. J. 1990. *Annu. Rev. Astron. Astrophys.* 28: 215–61
27. Dickey, J. M., Salpeter, E. E., Terzian, Y. 1978. *Ap. J. Suppl.* 36: 77–114
28. Dyson, J. E., Hartquist, T. W. 1987. *MNRAS* 228: 453–61
29. Edgar, R. J. 1986. *Ap. J.* 308: 389–400
30. Fabian, A. C., Canizares, C. R., Barcons, X. 1989. *MNRAS* 239: 15P–18P
31. Fichtel, C. E., Hartman, R. C., Kniffen, D. A., Thompson, D. J., Oegelman, H. B., et al. 1977. *Ap. J. Lett.* 217: L9–13
32. Fink, R. 1989. PhD thesis. Pa. State Univ., Univ. Park. 286 pp.
33. Fried, P. M. 1978. PhD thesis. Univ. Wisc., Madison. 183 pp.
34. Fried, P. M., Nousek, J. A., Sanders, W. T., Kraushaar, W. L. 1980. *Ap. J.* 242: 987–1004
35. Garmire, G. P., Nugent, J. J. 1981. *Bull. Am. Astron. Soc.* 13: 786–87 (Abstr.)
36. Giacconi, R., Gursky, H., Paolini, F. R., Rossi, B. B. 1962. *Phys. Rev. Lett.* 9: 439–43
37. Giacconi, R., Zamorani, G. 1987. *Ap. J.* 313: 20–27
38. Gorenstein, P., Tucker, W. H. 1972. *Ap. J.* 176: 333–44
39. Hamilton, T. T., Helfand, D. J. 1987. *Ap. J.* 318: 93–102
40. Hayakawa, S. 1973. In *X- and Gamma-Ray Astronomy, IAU Symp. No. 55*, ed. H. Bradt, R. Giacconi, pp. 235–49. Dordrecht: Reidel. 323 pp.
41. Hayakawa, S. 1979. See Ref. 2, pp. 323–35
42. Hayakawa, S., Kato, T., Nagase, F., Yamashita, K. 1979. *Publ. Astron. Soc. Jpn.* 31: 71–86
43. Hayakawa, S., Kato, T., Nagase, F., Yamashita, K., Murakami, T., Tanaka, Y. 1977. *Ap. J. Lett.* 213: L109–13
44. Hayakawa, S., Kato, T., Nagase, F., Yamashita, K., Tanaka, Y. 1978. *Astron. Astrophys.* 62: 21–28
45. Hearn, D. R., Richardson, J. A., Bradt, H. V. D., Clark, G. W., Lewin, W. H. G., et al. 1976. *Ap. J. Lett.* 203: L21–24
46. Heiles, C., Chu, Y., Reynolds, R. J., Yegingil, I., Troland, T. H. 1980. *Ap. J.* 242: 533–40
47. Helfand, D. J., Caillault, J.-P. 1982. *Ap. J.* 253: 760–67
48. Henry, R. C., Fritz, G., Meekins, J. F., Chubb, T., Friedman, H. 1971. *Ap. J. Lett.* 163: L73–77
49. Henry, R. C., Fritz, G., Meekins, J. F., Friedman, H., Byram, E. T. 1968. *Ap. J. Lett.* 153: L11–18
50. Innes, D. E., Hartquist, T. W. 1984. *MNRAS* 209: 7–13
51. Inoue, H., Koyama, K., Matsuoka, M., Ohashi, T., Tanaka, Y., Tsunemi, H. 1979. *Ap. J. Lett.* 227: L85–88
52. Inoue, H., Koyama, K., Matsuoka, M., Ohashi, T., Tanaka, Y., Tsunemi, H. 1980. *Ap. J.* 238: 886–91
53. Iwan, D. 1980. *Ap. J.* 239: 316–27
54. Iwan, D., Marshall, F. E., Boldt, E. A., Mushotzky, R. F., Shafer, R. A.,

Stottlemyer, A. 1982. *Ap. J.* 260: 111–23
55. Jahoda, K., McCammon, D. 1988. *Nucl. Instrum. Methods A* 272: 800–13
56. Jahoda, K., McCammon, D., Dickey, J. M., Lockman, F. J. 1985. *Ap. J.* 290: 229–37
57. Jahoda, K., McCammon, D., Lockman, F. J. 1986. *Ap. J. Lett.* 311: L57–61
58. Jakobsen, P., Kahn, S. M. 1986. *Ap. J.* 309: 682–93
59. Jenkins, E. B. 1978. *Ap. J.* 219: 845–60
60. Jenkins, E. B. 1978. *Ap. J.* 220: 107–23
61. Jenkins, E. B., Meloy, D. A. 1974. *Ap. J. Lett.* 193: L121–25
62. Juda, M. 1988. PhD thesis. Univ. Wisc., Madison. 130 pp.
63. Juda, M., Bloch, J. J., McCammon, D., Sanders, W. T., Snowden, S. L. 1987. *Bull. Am. Astron. Soc.* 19: 722 (Abstr.)
64. Kahn, S. M., Caillault, J.-P. 1986. *Ap. J.* 305: 526–33
65. Kahn, S. M., Jakobsen, P. 1988. *Ap. J.* 329: 406–9
66. Kato, T. 1976. *Ap. J. Suppl.* 30: 397–449
67. Koyama, K. 1989. *Publ. Astron. Soc. Jpn.* 41: 665–78
68. Koyama, K., Makishima, K., Tanaka, Y., Tsunemi, H. 1986. *Publ. Astron. Soc. Jpn.* 38: 121–31
69. Kraushaar, W. L. 1976. *Bull. Am. Astron. Soc.* 8(4): 548 (Abstr.)
70. Kraushaar, W. L. 1979. See Ref. 2, pp. 293–308
71. Kraushaar, W. L., Clark, G. W., Garmire, G. P., Borken, R., Higbie, P., et al. 1972. *Ap. J.* 177: 341–63
72. Kulkarni, S. R., Heiles, C. 1987. In *Interstellar Processes*, ed. D. J. Hollenbach, H. A. Thronson, pp. 87–122. Dordrecht: Reidel. 807 pp.
73. Labov, S., Bowyer, S. 1988. *J. Phys.* 49: C1-63–66
74. Lampton, M., Margon, B., Bowyer, S. 1976. *Ap. J.* 208: 177–90
75. Leiter, D., Boldt, E. 1982. *Ap. J.* 260: 1–18
76. Levine, A., Rappaport, S., Halpern, J., Walter, F. 1977. *Ap. J.* 211: 215–22
77. Long, K. S., Agrawal, P. C., Garmire, G. P. 1976. *Ap. J.* 206: 411–17
77a. Manchester, R. N., Lyne, A. G., Johnston, S., D'Amico, N., Lim, J., Kniffen, D. A. 1989. *IAU Circ. No. 4892*
78. Margon, B., Bowyer, S., Cruddace, R., Heiles, C., Lampton, M., Troland, T. 1974. *Ap. J. Lett.* 191: L117–19
79. Marshall, F. E., Boldt, E. A., Holt, S. S., Miller, R. B., Mushotzky, R. F., et al. 1980. *Ap. J.* 235: 4–10
80. Marshall, F. J., Clark, G. W. 1984. *Ap. J.* 287: 633–52
81. Mason, I. M. 1981. PhD thesis. Univ. College London, Engl. 372 pp.
82. Mason, I. M., Culhane, J. L. 1983. *IEEE Trans. Nucl. Sci.* NS-30: 485–90
83. McCammon, D., Bunner, A. N., Coleman, P. L., Kraushaar, W. L. 1971. *Ap. J. Lett.* 168: L33–37
84. McCammon, D., Burrows, D. N., Sanders, W. T., Kraushaar, W. L. 1983. *Ap. J.* 269: 107–35
85. McCammon, D., Meyer, S. S., Sanders, W. T., Williamson, F. O. 1976. *Ap. J.* 209: 46–52
86. McKee, C. F., Ostriker, J. P. 1977. *Ap. J.* 218: 148–69
87. Mewe, R., Gronenschild, E. H. B. M., van den Oord, G. H. J. 1985. *Astron. Astrophys. Suppl.* 62: 197–254
87a. Morisawa, K., Matsuoka, M., Takahara, F., Piro, L. 1989. *Proc. ESLAB Symp. X-Ray Astron., 23rd.* In press
88. Morrison, R., McCammon, D. 1983. *Ap. J.* 270: 119–22
89. Moseley, S. H., Mather, J. C., McCammon, D. 1984. *J. Appl. Phys.* 56: 1257–62
90. Naranan, S., Shulman, S., Friedman, H., Fritz, G. 1976. *Ap. J.* 208: 718–26
91. Nousek, J. A., Burrows, D. N., Good, J., Singh, K. P. 1986. *Bull. Am. Astron. Soc.* 18: 1029 (Abstr.)
92. Nousek, J. A., Fried, P. M., Sanders, W. T., Kraushaar, W. L. 1982. *Ap. J.* 258: 83–95
93. Pallavicini, R., ed. 1988. *Hot Thin Plasmas in Astrophysics*. Dordrecht: Kluwer. 434 pp.
94. Palmieri, T. M., Burginyon, G. A., Grader, R. J., Hill, R. W., Seward, F. D., Stoering, J. P. 1971. *Ap. J.* 169: 33–39
95. Paresce, F. 1984. *Astron. J.* 89(7): 1022–37
96. Penzias, A. A., Wilson, R. W. 1965. *Ap. J.* 142: 419–21
97. Policarpo, A. J. P. L. 1977. *Space Sci. Instrum.* 3: 77–107
98. Raymond, J. C. 1988. See Ref. 93, pp. 3–20
99. Raymond, J. C., Smith, B. W. 1977. *Ap. J. Suppl.* 35: 419–39
99a. Raymond, J. C., Smith, B. W. 1984. Informally distributed update to Ref. 99
100. Reynolds, R. J. 1989. *Ap. J. Lett.* 339: L29–32
101. Reynolds, R. J., Ogden, P. M. 1979. *Ap. J.* 229: 942–53
102. Ride, S. K., Walker, A. B. C. Jr. 1977. *Astron. Astrophys.* 61: 347–52
103. Rocchia, R., Arnaud, M., Blondel, C., Cheron, C., Christy, J. C., et al. 1984. *Astron. Astrophys.* 130: 53–61

104. Rosner, R., Avni, Y., Bookbinder, J., Giacconi, R., Golub, L., et al. 1981. *Ap. J. Lett.* 249: L5–9
105. Rothenflug, R. 1988. See Ref. 93, pp. 197–211
106. Rothschild, R., Boldt, E., Holt, S., Serlemitsos, P., Garmire, G., et al. 1979. *Space Sci. Instrum.* 4: 269–301
107. Ryter, C., Cesarsky, C. J., Audouze, J. 1975. *Ap. J.* 198: 103–9
108. Sanders, W. T. 1976. PhD thesis. Univ. Wisc., Madison. 134 pp.
109. Sanders, W. T., Burrows, D. N., McCammon, D., Kraushaar, W. L. 1983. In *Supernova Remnants and Their X-Ray Emission, IAU Symp. No. 101*, ed. J. Danziger, P. Gorenstein, pp. 361–65. Dordrecht: Reidel. 614 pp.
110. Sanders, W. T., Kraushaar, W. L., Nousek, J. A., Fried, P. M. 1977. *Ap. J. Lett.* 217: L87–91
111. Sanders, W. T., Snowden, S. L., Edgar, R. J. 1990. In *High Resolution X-Ray Spectroscopy of Cosmic Plasmas*, ed. P. Gorenstein, M. V. Zombeck. Cambridge: Univ. Press. In press
112. Schnopper, H. W., Delvaille, J. P., Rocchia, R., Blondel, C., Cheron, C., et al. 1982. *Ap. J.* 253: 131–35
113. Schwartz, D. A. 1979. See Ref. 2, pp. 453–65
114. Schwartz, D. A., Gursky, H. 1974. In *X-Ray Astronomy*, ed. R. Giacconi, H. Gursky, pp. 359–88. Dordrecht: Reidel. 450 pp.
115. Schwartz, H. E., Mason, I. M. 1984. *Nature* 309: 532–34
116. Setti, G. 1989. *Proc. Yamada Conf. XX: Big Bang, Active Galactic Nuclei, and Supernovae*. In press
117. Shafer, R. A. 1983. PhD thesis. Univ. Md., College Park. *NASA Tech. Memo. 85029*. 471 pp.
118. Shapiro, P. R., Field, G. B. 1976. *Ap. J.* 205: 762–65
119. Shapiro, P. R., Moore, R. T. 1976. *Ap. J.* 207: 460–83
120. Siegmund, O. H. W., Clothier, S., Culhane, J. L., Mason, I. M. 1982. *IEEE Trans. Nucl. Sci.* NS-30: 350
120a. Slavin, J. D. 1989. *Ap. J.* 346: 718–27
121. Snowden, S. L., Cox, D. P., McCammon, D., Sanders, W. T. 1990. *Ap. J.* 354: 211–19
122. Spitzer, L. 1956. *Ap. J.* 124: 20–34
123. Stern, R., Wang, E., Bowyer, S. 1978. *Ap. J. Suppl.* 37: 195–222
124. Tanaka, Y., Bleeker, J. A. M. 1977. *Space Sci. Rev.* 20: 815–88
125. Truemper, J. 1986. In *Cosmic Radiation in Contemporary Astrophysics*, ed. M. M. Shapiro, pp. 241–47. Dordrecht: Reidel. 274 pp.
126. Turner, M. J. L., Thomas, H. D., Patchett, B. E., Reading, D. H., Makishima, K., et al. 1989. *Publ. Astron. Soc. Jpn.* 41: 345–72
127. van den Heuvel, E. P. J., Rappaport, S. 1987. In *Physics of Be Stars*, ed. A. Slettebak, T. P. Snow, pp. 291–308. Cambridge: Univ. Press. 557 pp.
128. Vanderhill, M. J., Borken, R. J., Bunner, A. N., Burstein, P. H., Kraushaar, W. L. 1975. *Ap. J. Lett.* 197: L19–22
129. Warwick, R. S., Pye, J. P., Fabian, A. C. 1980. *MNRAS* 190: 243–60
130. Warwick, R. S., Turner, M. J. L., Watson, M. G., Willingale, R. 1985. *Nature* 317: 218–21
131. Weymann, R. 1967. *Ap. J.* 147: 887–900
132. Williamson, F. O., Sanders, W. T., Kraushaar, W. L., McCammon, D., Borken, R., Bunner, A. N. 1974. *Ap. J. Lett.* 193: L133–37
133. Worrall, D. M., Marshall, F. E., Boldt, E. A., Swank, J. H. 1982. *Ap. J.* 255: 111–21
134. Zhang, J., Edwards, B., Juda, M., Kelley, R., Madejski, G., et al. 1990. In *High Resolution X-Ray Spectroscopy of Cosmic Plasmas*, ed. P. Gorenstein, M. V. Zombeck. Cambridge: Univ. Press. In press